

Supplementary Materials

Materials and Methods

Human Subjects. All patients were enrolled in clinical trial (NCT00683670, BB-IND 13590) and signed informed consents that had been approved by the Institutional Review Board of Washington University. All subjects were HLA-A*02:01+, had no evidence of autoimmune disorder and were negative for HIV, HBV, and HCV. Leukapheresis was performed, prior to treatment and after the 3rd mature dendritic cell (DC) vaccination, at Barnes Jewish Hospital blood bank. Patients were not prescreened for interleukin (IL)-12p70 DC production prior to treatment. Prior to treatment, baseline imaging was performed by MRI scan of brain and CT scan of the chest /abdomen /pelvis with i.v. contrast. Toxicities and adverse effects were graded according to the National Cancer Institute Common Toxicity Scale (version 3.0). A detailed patient description is given in Supplementary Text section.

Tissue procurement and nucleic acid isolation. Informed consent for genome sequencing was obtained for all patients on a protocols approved by the Institutional Review Board of Washington University. All tumor samples were flash frozen except one from MEL 21 (skin, 6/06/2013), which was formalin-fixed paraffin embedded. Peripheral blood mononuclear cells (PBMC) were cryopreserved as cell pellets. DNA samples were prepared using QIAamp DNA Mini Kit (Qiagen) and RNA using High Pure RNA Paraffin kit (Roche). DNA and RNA quality was determined by Nanodrop 2000 and quantitated by the Qubit Fluorometer (Life Technologies).

Genomic Analysis: Exome sequencing. For each patient, tumor/PBMC (normal) matched genomic DNA samples were processed for exome sequencing with one normal and two tumor libraries, each using 500 ng DNA input (31). Exome sequence data was generated as 2 x 100 bp read pairs on an Illumina HiSeq2000 instrument and alignment of exome reads was performed using our Genome Modeling System (GMS) processing-profile. This pipeline uses BWA (version 0.5.9) for alignment with default parameters except for the following: ‘-t 4 -q 5’. All alignments were against GRCh37-lite-build37 of the

human reference genome and were merged and subsequently de-duplicated with Picard (version 1.46). Detection of somatic mutations was performed using the union of three variant callers: 1) SAMtools version r963 (params: -A -B) filtered by snp-filter v1 and further intersected with Somatic Sniper version 1.0.2 (params: —F vcf q 1 -Q 15) and processed through false-positive filter v1 (params: --bam-readcount-version 0.4 --bam-readcount-min-base-quality 15 --min-mapping-quality 40 --min-somatic-score 40) 2) VarScan Somatic version 2.2.6 filtered by varscan-high-confidence filter version v1 and processed through false-positive filter v1 (params: --bam-readcount- version 0.4 --bam-readcount-min-base-quality 15), and 3) Strelka version 1.0.10 (params: isSkipDepthFilters = 1). Amino acid substitutions (AAS) corresponding to each of the coding missense mutations (MM) were translated into a 21-mer amino acid FASTA sequence, with ideally 10 amino acids flanking the substituted amino acid on each side. Each 21-mer amino acid sequence was then evaluated through the HLA class I peptide binding algorithm NetMHC 3.4 to predict high affinity HLA-A*02:01 nonamer peptides for the AAS- as well as the WT sequence to calculate differences in binding affinities (8, 32). Any peptides with binding affinity IC50 value < 500nm were considered for further analysis.

cDNA-capture sequencing. All RNA samples were DNase-treated with TURBO DNA-free kit (Invitrogen) as per manufacturer's instructions; RNA integrity and concentration were assessed using Agilent Eukaryotic Total RNA 6000 assay (Agilent Technologies) and Quant-iT™ RNA assay kit on a Qubit™ Fluorometer (Life Technologies Corporation). Given the dynamic nature of genomic technologies, multiple overlapping methods were tested. However, results for tumors within a patient (Tables S1-S3) are consistent with one methodology: NuGen Ovation V2 for MEL38 and MEL218, Illumina TruSeq Stranded for MEL21. The MicroPoly(A)Purist™ Kit (Ambion) was used to enrich for poly(A) RNA from MEL218 and MEL38 DNase-treated total RNA; MEL21 RNA was ribo-depleted using the Ribo-Zero™ Magnetic Gold Kit (EpiCentre, Madison WI) following the manufacturer protocol. We used either the Ovation® RNA-Seq System V2 (NuGen, 20 ng of either total or polyA RNA), or the Ovation® RNA-Seq FFPE System (NuGen, 150 ng of DNase-treated total RNA) or the TruSeq Stranded Total RNA Sample Prep kit (Illumina, 20 ng ribosomal RNA-depleted total RNA) for cDNA

synthesis. All NuGen cDNA sequencing libraries were generated using NEBNext® Ultra™ DNA Library Prep Kit for Illumina® with minor modifications. All NuGEN generated cDNA was processed as described previously (9). Briefly, 500 ng of cDNA was fragmented, end-repaired, and adapter-ligated using IDT synthesized “dual same index” adapters. The TruSeq stranded cDNA was also end-repaired and adapter-ligated using IDT synthesized “dual same index” adapters. These indexed adapters, similar to Illumina TruSeq HT adapters, contain the same 8 bp index on both strands of the adapter. Binning reads requires 100% identity from the forward and reverse indexes to minimize sample crosstalk in pooling strategies. Each library ligation reaction was PCR-optimized using the Eppendorf Epigradient S qPCR instrument, and PCR-amplified for limited cycle numbers based on the Ct value in the optimization step. Libraries were assessed for concentration using the Quant-iTTM dsDNA HS Assay (Life Technologies) and for size using the BioAnalyzer 2100 and the Agilent DNA 1000 Assay (Agilent Technologies). The Illumina-ready libraries were enriched using the Nimblegen SeqCap EZ Human Exome Library v3.0 reagent. The targeted genomic regions in this kit cover 63.5 Mb or 2.1% of the human reference genome, including 98.8% of coding regions, 23.1% of untranslated regions (UTRs), and 55.5% of miRNA bases (as annotated by Ensembl version 73 (33)). Each hybridization reaction was incubated at 47° C for 72 hours, and single-stranded capture libraries were recovered and PCR-amplified per the manufacturer’s protocol. Post-capture library pools were sized and mixed at a 1:0.6 sample:AmpureXP magnetic bead ratio to remove residual primer-dimers and to enrich for a library fragment distribution between 300 and 500bp. The pooled capture libraries were diluted to 2 nM for Illumina sequencing. For cDNA-capture data were aligned with Tophat v2.0.8 (params: --bowtie-version=2.1.0 for Ovation; --library-type fr-firststrand --bowtie-version=2.1.0 for Truseq). For Ovation data, prior to alignment, paired 2x100 bp sequence reads were trimmed with flexbar v 2.21 (params: --adapter CTTTGTGTTGA - -adapter-trim-end LEFT --nono-length-dist --threads 4 --adapter-min-overlap 7 --max-uncalled 150 --min-readlength 25) to remove single primer isothermal amplification adapter sequences. Expression levels (FPKM) were calculated with Cufflinks v2.0.2 (params--max-bundle-length=10000000--num-threads 4). A visual review step of cDNA capture data was performed to evaluate for expression of MM identified by exome data.

Both cDNA-capture (Alt-read number) and FPKM values were considered for candidate prioritization.

Peptides: Peptides were obtained lyophilized from American Peptide Company (>95% purity), dissolved in 10% DMSO in sterile water and tested for sterility, purity, endotoxin and residual organics. Peptide binding to HLA-A*02:01 was determined by T2 assay (10) or using the fluorescence polarization assay (Pure Protein, L.L.C.) (11). The affinity scale of this latter assay is: high binders: log (IC₅₀ nM) <3.7; intermediate binders: log (IC₅₀ nM) 3.7-4.7; low binders: log (IC₅₀ nM) 4.7-5.5; and very low binders: log (IC₅₀ nM) ≥6.0 (11).

DC manufacturing and vaccine: Cyclophosphamide (300 mg/m²) was given 96 h prior to the first DC dose with the intention of eliminating Tregs. All mature DC (mDC) vaccine doses were prepared at time of immunization from either freshly isolated (D1) or cryopreserved (D2-3) PBMC (all derived from same leukapheresis collection). For each vaccine dose, monocyte-derived immature DCs were generated in 100 ng/mL granulocyte-macrophage colony-stimulating factor (GM-CSF, Berlex) and 20 ng/mL IL-4 (Miltenyi Biotec) as described (7). Six days after culture initiation, immature DCs were cultured with irradiated (10,000 rad) GMP-grade CD40L-expressing K562 cells (7), 100 u/mL IFN-γ (Actimmune, InterMune Inc.), poly I:C (Invivogen, Inc) and R848 (Invivogen, Inc.) for 16h to generate mDC. Two hours prior to infusion, mDC were pulsed (50 ug/10⁶ cells/mL) separately with each peptide (7 AAS-peptides and 2 gp100 peptides, G209-2M and G280-9V) and, for dose 1 only, influenza virus vaccine (Fluvirin, Novartis) was added to provide a source of recall antigen for CD4+ T cells. IL-12p70 production by vaccine DC was measured by ELISA (eBioscience) in accordance to the manufacturer's instructions. The initial priming dose was 1.5x10⁷ DC per peptide (1.35x10⁸ DC total), in remaining doses, patients received 5x10⁶ DC per peptide (4.5x10⁷ DC total). mDC were resuspended in 50 mL normal saline supplemented with 5% human serum albumin and administered over 30 min by intravenous infusion after pre-medication with acetaminophen 650 mg. The purpose of this trial was to determine the

safety, tolerability and immunological responses to AAS-peptides formulated in a mDC vaccine. Patients underwent clinical evaluation prior to each mDC infusion.

Immunologic monitoring and dextramer assay: Immunologic analysis to evaluate the kinetic and magnitude of T cell response to AAS-encoding and gp100-derived peptides was performed using PBMC collected weekly as described (7). Briefly, fresh PBMC obtained by Ficoll-Paque PLUS gradient centrifugation were cultured with 40 ug/mL peptide and IL-2 (50U/mL). On day 10 (peak of response, unpublished data), neoantigen-specific T cell frequencies were determined by staining with HLA-A*02:01/peptide dextramers (Immudex), followed by addition of FITC-CD4, -CD14, -CD19 (Invitrogen) and Alexa 488-CD56 (BD Pharmigen), APC-CD8 (Invitrogen). Cells were washed, resuspended in FACS buffer containing 7AAD. Twenty five thousand events in the CD8+ gate were collected using a hierarchical gating strategy that included FSC/SSC and excluded 7AAD-positive (dead cells) and CD4/14/19/56-positive cells. PBMC / CD8+ T cells derived from an unrelated HLA-A*02:01 patient were used as negative controls for assessing specificity of HLA-A*02:01/AAS-peptide dextramers (data not shown). Data was acquired and analyzed using Flow-Jo software.

Analysis of T cell responses: For functional characterization, neoantigen-specific T cell lines were generated using autologous mDC and antigen loaded artificial antigen presenting cells at a ratio of 1:1 as previously described (12); antigen-specific frequencies in T cell lines are shown in Fig. S4B. To determine the peptide avidity (effective concentration at 50% maximal lysis, EC₅₀) of neoantigen-specific T cells, T2 cells were pulsed with titrated peptide concentrations for 1h, followed by ⁵¹Cr (25uCi) labeling for 1 h, washed twice and tested in a standard 4h ⁵¹Cr release assay using neoantigen-specific T cells as effectors. For production of cytokines, neoantigen-specific T cells were re-stimulated using artificial antigen presenting cells in the presence or absence of peptide, supernatants collected at 24h and cytokine produced determined using MILLIPLEX® MAP Human Cytokine Panel I (EMD Millipore).

Tandem mini-gene constructs (TMC) and antigen processing: TMC consisting of 7-10 minigenes (Table S5) were cloned into pMX (GFP+), expressed as retrovirus and used to transduced the HLA-A*02:01+ melanoma lines DM6 or A375 (obtained from ATCC and mycoplasma free). TMC expressing cells were selected by sorting for GFP+ cells expressing cell surface HLA-A*02:01/SVG9 peptide complexes as detected by a T cell receptor mimic (TCRm) monoclonal antibody(34). AAS- and WT-TMC reactivity with the HLA-A*02:01/SVG9 peptide complex specific TCRm monoclonal antibody validated expression of the mini-gene constructs. DM6 cells expressing TMC were labeled with 25uCi ^{51}Cr for 1h, washed and tested as targets in a standard 4h assay using neoantigen-specific T cells as effectors (12). DM6 cells expressing TMC were co-cultured with neoantigen-specific T cells at a 1:1 ratio, supernatants harvest at 16 h, and IFN- γ production evaluated by ELISA as described (12).

Proteomic Analysis: Production and Isolation of HLA-A*02:01/ Peptide Complexes. TMC expressing A375 melanoma cells were transfected with soluble HLA-A*02:01 (sHLA-A*02:01) and single cell sorted for a high (>1000 ng/ml in static culture) sHLA-A*02:01 producing clone. The sHLA-A*02:01 construct includes a C-terminal VLDLr epitope purification tag (SVVSTDDDLA) that is recognized by the anti-VLDLr mAb (ATCC CRL-2197). This antibody was also used for quantification of sHLA production as the capture antibody in a sandwich ELISA, with an antibody directed against β 2-microglobulin (Dako Cytomation) as the detector antibody. Cells were grown in roller bottles and sHLA/peptide complexes were purified from supernatants by affinity chromatography with the anti-VLDLr antibody (35). Eluate fractions containing sHLA/peptide complexes were brought to a final acetic acid concentration of 10%, pooled, and heated to 78°C in a water bath. Peptides were purified through a 3 kDa molecular weight cutoff cellulose membrane (EMD Millipore) and lyophilized.

Mass spectrometric analysis. Synthetic peptides corresponding to the mutant sequences were resuspended in 10% acetic acid in water at 1 μM , and fractionated by RP-HPLC with an acetonitrile gradient in 10 mM ammonium formate at pH 10. Peptide-containing fractions were dried and resuspended in 25 ul of 10% acetic acid and subjected to nano-scale RP-HPLC at pH 2.5 utilizing an Eksigent nanoLC coupled to a TripleTOF 5600

(AB Sciex) quadrupole time-of-flight mass spectrometer (LC/MS). Information dependent acquisition (IDA) was used to obtain MS and MS/MS fragment spectra for peptide ions. The sequence of each peptide was determined by observed mass and fragment ions, and the 1st dimension fraction number and LC/MS retention times were recorded.

Next, peptides purified from TMC expressing A375 melanoma cells were resuspended in 10% acetic acid and HPLC fractionated under the same conditions and gradient method. The HPLC fractions corresponding to those containing the synthetic peptides were then subjected to the same LC/MS conditions. Resulting spectra were found positive for the presence of the mutant peptides if the following criteria were met: 1. The observed fragment ions were in the same RP-HPLC fraction as the synthetic, 2. LC/MS elution time was within 2 minutes of the synthetic, and 3. Fragment ion masses matched those of the synthetic with an accuracy of \pm 25 ppm. PeakView® Software version: 1.2.0.3 was used for exploring and interpreting of the LC/MS data.

Instrument parameters and gradient methods. Separation and sequencing of peptides were carried out by two-dimensional liquid chromatography, followed by information-dependent acquisition (IDA) generated tandem MS (MS/MS). For the first dimension, the peptide sample was loaded on a reverse-phase C₁₈ column (pore size, 110 Å; particle size, 5 µm; 2 mm i.d. by 150 mm long Gemini column; Phenomenex) with a Michrom BioResources Paradigm MG4 high performance liquid chromatograph (HPLC) with UV detection at 215 nm wavelength. Elution was at pH 10 using 10 mM ammonium formate in 2% acetonitrile/98% water as solvent A and 10 mM ammonium formate in 95% acetonitrile/5% water for solvent B. The 1st dimension HPLC column was pre-equilibrated at 2% solvent B, then the peptide sample, dissolved in 10% acetic acid/water, was loaded at a flow rate of ~120 µl/min over an 18 minute period. Then a two segment gradient was performed at 160 µl/min; the 1st segment was a 40 minute linear gradient from 4% B to 40% B, followed by an eight minute linear gradient from 40% B to 80% B. Forty peptide-rich fractions were collected and dried by vacuum centrifugation.

For the second dimension chromatography, each dried fraction was resuspended in 10% acetic acid and subjected to nano-scale RP-HPLC (Eksigent nanoLC415, AB Sciex). The second dimension nano-HPLC setup included a C₁₈ trap column (350 µm i.d. by 0.5 mm

long; ChromXP) with 3 μ m particles and 120 \AA pores and a ChromXP, C₁₈ separation column with dimensions of 75 μ m i.d. by 15 cm long packed with the same medium. A two-solvent system was utilized, where solvent A is 0.1% formic acid in water and solvent B contains 0.1% formic acid in 95% acetonitrile/5% water. Samples were loaded at 5 μ L/min flow rate on the trap column and at 300 nL/min flow rate on the separation column that was equilibrated in 2% solvent B. The separation was performed by a program with two linear gradients: 10% to 40% solvent B for 70 min and then 40% to 80% solvent B for 7 min. The column effluent was connected to the nanospray III ion source of an AB Sciex TripleTOF 5600 quadrupole-time of flight mass spectrometer with the source voltage set to 2400 v.

Information dependent analysis (IDA) of peptide ions was performed utilizing a survey scan in the TOF-MS positive-ion mode over a mass range of 300 m/z to 1250 m/z in 250 milliseconds. Observed ions with a charge state of 2 to 5 and an ion intensity of at least 200 counts, were subjected to collision-induced dissociation (CID). For each survey scan, up to 22 ions were subjected to CID analysis over a maximum period of 3.3 seconds. Selection of ion m/z was excluded for 30 seconds after 3 initial MS/MS experiments. Dynamic collision energy was utilized to automatically adjust the collision voltage based upon the ion size and charge. PeakView® Software version: 1.2.0.3 was used for exploring and interpreting of the data.

TCR β Repertoire Analysis: Short-term ex-vivo expanded neoantigen-specific T cells were purified to 97-99% purity by cell sorting in a Sony SY3200 BSC (Sony Biotechnology) fitted with a 100 μ m nozzle, at 30 psi, using 561nm (585/40) and 642nm (665/30) lasers and cell pellets were prepared. DNA isolation and TCR β sequencing was performed by Adaptive Biotechnologies and The Genome Institute at Washington University. Sequencing was performed at either survey (for neoantigen-specific TCR β reference libraries) or deep (for pre- and post-vaccine CD8+ T cell populations) level (22, 36). TCR β V-, D-, J- genes of each CDR3 regions were defined using IMGT (ImMunoGeneTics)/Junctional algorithms and data uploaded into the ImmunoSeq Analyzer (Adaptive Biotechnologies) for analysis. Complete amino acid identity between reference library and pre- and post-vaccine CD8 samples was required for assigning a

TCR β match. In reference library, TCR β clonotypes with frequencies above 0.1% (>100-fold sequencing depth) were set as a threshold for identification of neoantigen-specific TCR β CDR3 sequences within pre- and post-vaccine CD8+ T cell populations. TCR β V-, D-, J- gene families, CDR3 amino acid sequences, frequencies and read counts for each T cell clonotype that matched reference library and pre- and post-vaccine CD8 populations are shown in Tables S6 - S10.

Supplementary Text

Patient Information

Patient MEL21 was a 54-year-old man diagnosed with stage 3C cutaneous melanoma of the right lower extremity in 2010. The BRAF V600E mutation was detected. Surgery was performed to excise 2cm inguinal lymph node and numerous in transit metastases. He developed recurrent in transit metastases and deep pelvic adenopathy in May 2012 and was given ipilimumab (3 mg/kg x 4 doses) with stable disease until late 2013. Disease progression was noted with increasing 2 cm external iliac, 1.2 cm inguinal, and 7 mm retrocrural adenopathy. Three surgically resected melanoma lesions (inguinal lymph node 1/30/11, leg skin 5/10/12, leg skin 6/6/13) and PBMC were submitted for genomic analysis in order to identify somatic missense mutations. The patient provided written informed consent for the study and underwent apheresis, and received cyclophosphamide 4 days prior to administration of the first vaccine dose. He received a total of three vaccine doses without side effect or toxicity. Re-staging CT showed stable disease and he remains in follow up 9 months later.

Patient MEL38 was a 47-year-old woman diagnosed with stage 3C cutaneous flank melanoma and underwent surgical resection of an axillary lymph node in 2012. The BRAF V600E mutation was detected. She developed recurrent disease in the skin and axilla that was surgically resected. A few months later, CT imaging confirmed metastatic disease in the right lung and axilla and she was given ipilimumab (3 mg/kg x 4 doses) in May 2012 with complications of grade 2 autoimmune colitis requiring prednisone taper and later, grade 3 hypophysitis requiring replacement therapy with levothyroxine and hydrocortisone. Disease progression was noted 12 months later with new lung and skin

metastases. Vemurafenib was administered for two months with no response in August 2013. Three surgically resected melanoma lesions (axilla lymph node 4/19/12, skin breast 2/14/13, skin abdominal wall 4/16/13) and PBMC were submitted for genomic analysis in order to identify somatic missense mutations. Further disease progression was evident with 3 lung nodules measuring 12 mm, 5 mm, and 5 mm in diameter. The patient provided written informed consent for the study and underwent apheresis, and received cyclophosphamide 4 days prior to the first vaccine dose. She received a total of three vaccine doses without side effect or toxicity. Re-staging CT showed 30% tumor reduction; however, the following CT examination 12 weeks later showed interval increase of tumor size back to baseline dimensions with no new sites of disease. The patient remains with stable disease for the past 8 months.

Patient MEL218 was a 52-year-old man diagnosed with stage 3C cutaneous melanoma on the left lower extremity in 2005. The BRAF mutation V600E mutation was detected when tested later on archived tumor. He underwent surgical resection and received adjuvant interferon for 6 months but had disease recurrence that was surgically resected on several occasions. In 2008, he developed disease progression with extensive in transit and subcutaneous metastases on the left leg with bulky inguinal nodal metastasis deemed unresectable. He received ipilimumab (10 mg/kg x 14 doses) on clinical trial from 2008-2012 with complete response. One surgical specimen (inguinal lymph node 4/4/05) and PBMC were submitted for genomic analysis to identify somatic missense mutations. The patient provided written informed consent for the study and underwent apheresis, and received cyclophosphamide 4 days prior to the first vaccine dose. He received a total of three vaccine doses administered in the adjuvant setting without side effect or toxicity. Re-staging PET-CT imaging confirms no evidence of recurrent or metastatic disease. The patient remains in complete remission and continues in follow up.

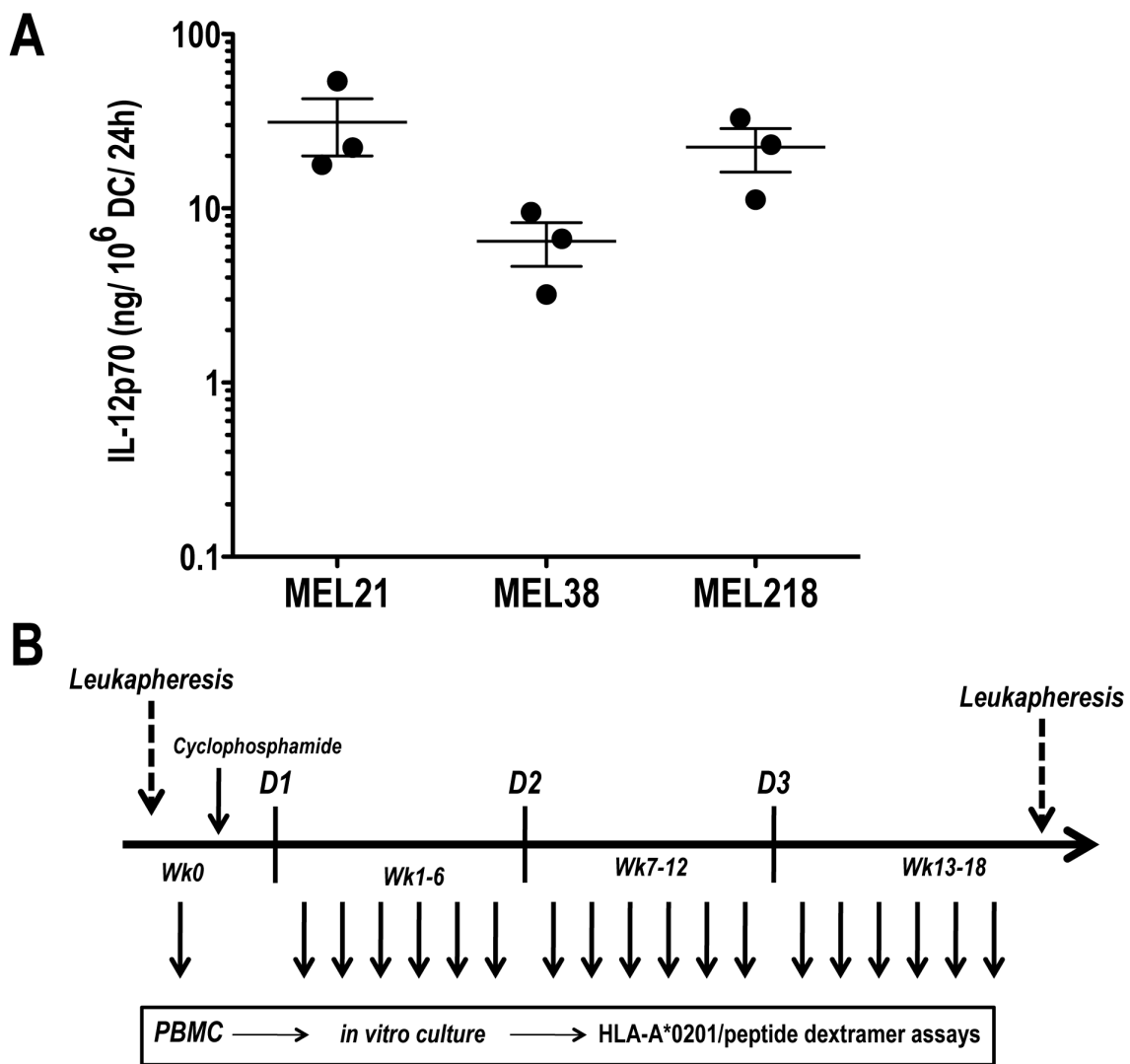


Fig. S1 Clinical trial schema and ex-vivo IL-12p70 levels produced by mature DC. (A) Dendritic cells (DC) were matured with CD40L, IFN- γ plus TLR3 (poly I:C) and TLR8 (R848) agonists in order to optimize the production of IL-12p70. Results shown are the ex-vivo IL-12p70 levels produced by patient-derived mature DC used for manufacturing vaccines doses D1-D3 (each symbol represents a vaccine dose). DC supernatants were harvested 24h after activation and IL-12p70 production levels determined by ELISA. Results represent mean \pm SEM. (B) Study timelines depicting cyclophosphamide treatment (300 mg/m^2 i.v), DC vaccinations (D1-D3), PBMC sampling for immune monitoring and leukapheresis collections. The vaccine dosing schedule was altered from every 3 weeks to every 6 weeks based on the kinetics of the T cell response seen in our earlier study (7).

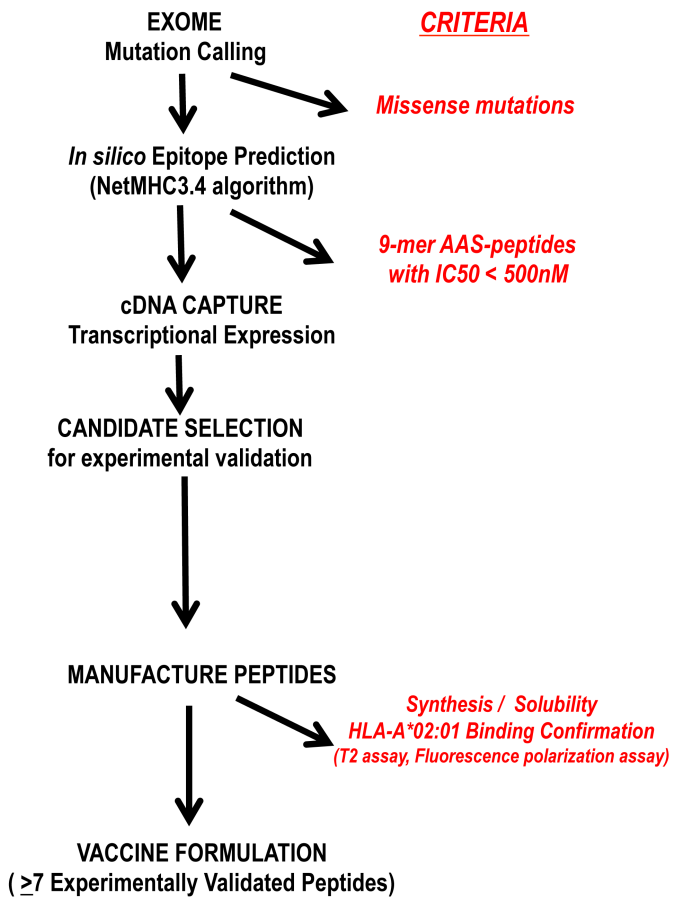
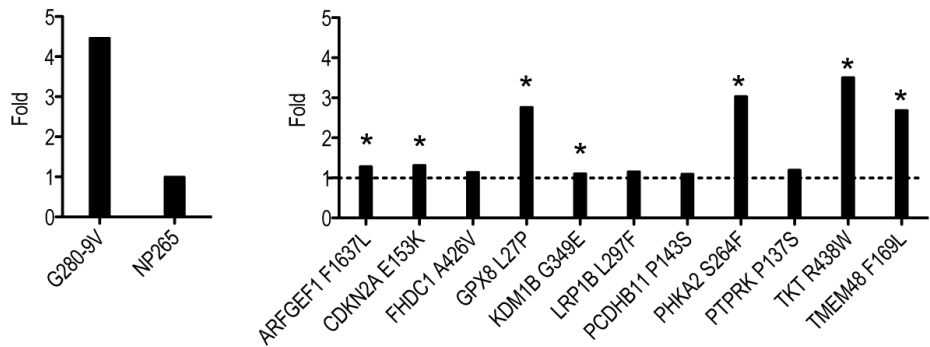
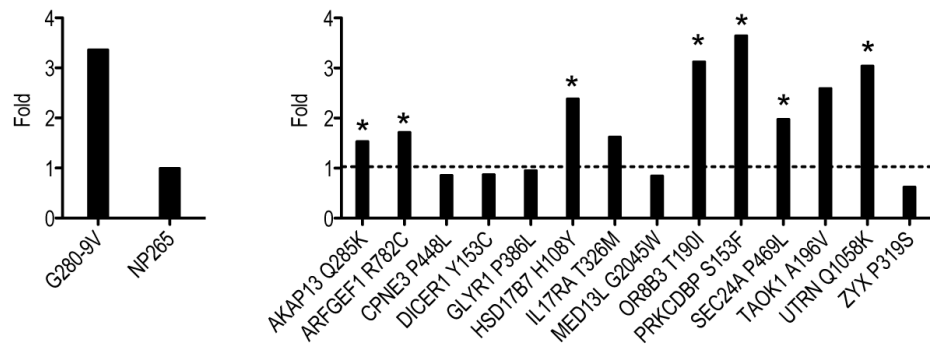


Fig. S2 Schematic representation of strategy for neoantigen selection. Tumor-specific missense mutations (MM) in melanoma samples were detected using exome sequencing and identified using the union of three variant calling algorithms. BRAF allelic frequency (Tables S1-S3) was considered the upper limit variant allelic fraction for each tumor and used as a comparator to assess the clonality of other MM-encoding genes. Amino acid substitutions (AAS) corresponding to each of the coding MM were translated into a 21-mer amino acid FASTA sequence and evaluated through the HLA class I peptide binding algorithm NetMHC 3.4 to predict HLA-A*02:01 nonamer AAS-encoding peptides with EC₅₀<500nM. Transcriptional status of genes encoding AAS candidates was determined by cDNA-capture and their expression levels determined using Cufflinks. Filters were applied to deprioritize those with low cDNA-capture (Alt_reads <5) and prioritize those with high numbers of Alt_reads and/or FPKM>1. For MEL21 and MEL38 patients, candidates were prioritized if expressed by more than one metachronous tumor. For experimental validation, candidates were further prioritized on the basis of predicted HLA-A*02:01 binding affinity and/or HLA-A*02:01 affinity differential between AAS- and WT- peptide (Tables S1-S3). Only those peptides with confirmed HLA-A*02:01 binding as determined by T2 assay (Fig. S3) and fluorescence polarization assay [log (IC₅₀ nM) <4.7, Table S4] were prioritized for vaccine formulation.

MEL21



MEL38



MEL218

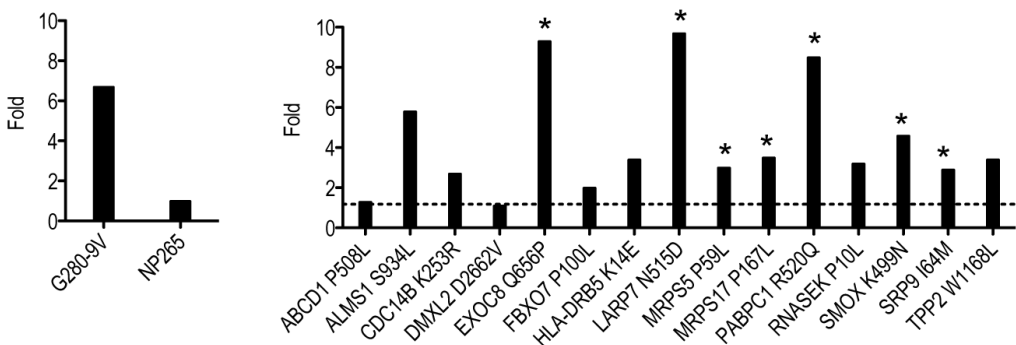


Fig. S3 AAS-encoding peptide binding to HLA-A*02:01. T2 cells were incubated with 100uM of the indicated peptide for 16 h, washed and stained with PE-conjugated anti-HLA-A*02:01 (clone BB7.2) monoclonal antibody. Melanoma G280-9V and Influenza NP265 peptides represent positive and negative controls, respectively. Binding fold are calculated as MFI experimental peptide / MFI NP265 peptide. Data are representative of 3 independent experiments. Peptides selected for incorporation in the vaccine formulation are indicated with an asterisk.

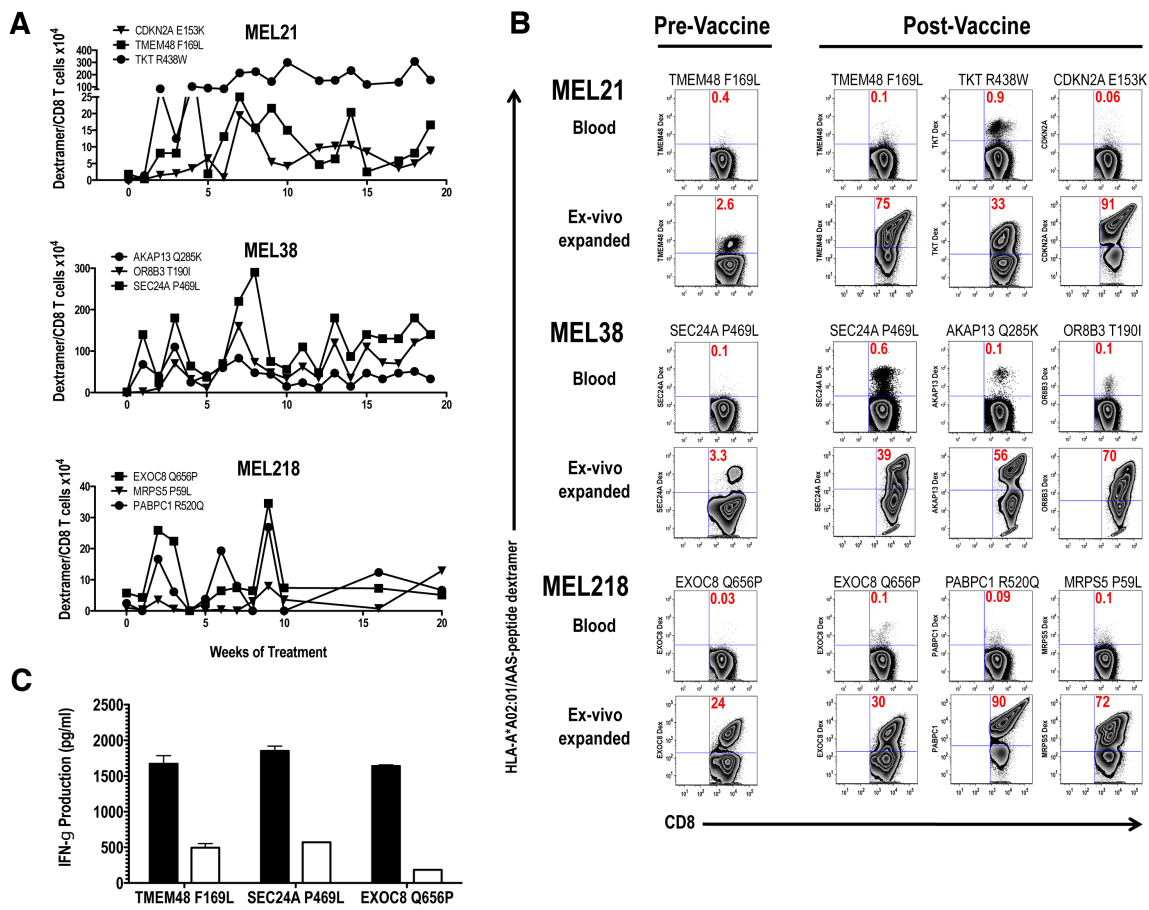


Fig. S4 Immunity to neoantigens. **(A)** Kinetics of immune responses to neoantigens. Time is recorded in weeks (0 indicates pre-vaccination). Culture conditions and staining details are described in Materials and Methods. Antigen-specific numbers were calculated based on dextramer percentage and total live cell yields. **(B)** Frequency of neoantigen specific T cells in CD8+ populations isolated directly from PBMC samples and after ex-vivo expansion using autologous DC and artificial antigen presenting cells. For dominant neoantigens TMEM48 F169L, SEC24A P469L and EXOC8 Q656, results are shown for samples obtained before vaccination (Pre-vaccine) and after 3 vaccine doses (Post-vaccine). For remaining neoantigens, results obtained with post-vaccine PBMC samples are shown. Percentage of neoantigen-specific CD8+ T cells is indicated in the right upper quadrant of the plot. A representative experiment of 2 performed is shown. **(C)** Ex-vivo expanded pre-vaccine neoantigen-specific T cells (dextramer % shown in Fig. S4B) were stimulated with artificial antigen presenting cells in the presence (closed bar) or absence (open bar) of AAS-peptide and supernatants were harvested at 24h. IFN- γ production was determined using ELISA assay. Mean values +/- standard deviation (SD) of duplicates are shown. Cytokine production by T cells in the absence of any stimuli was \leq 100 pg/mL.

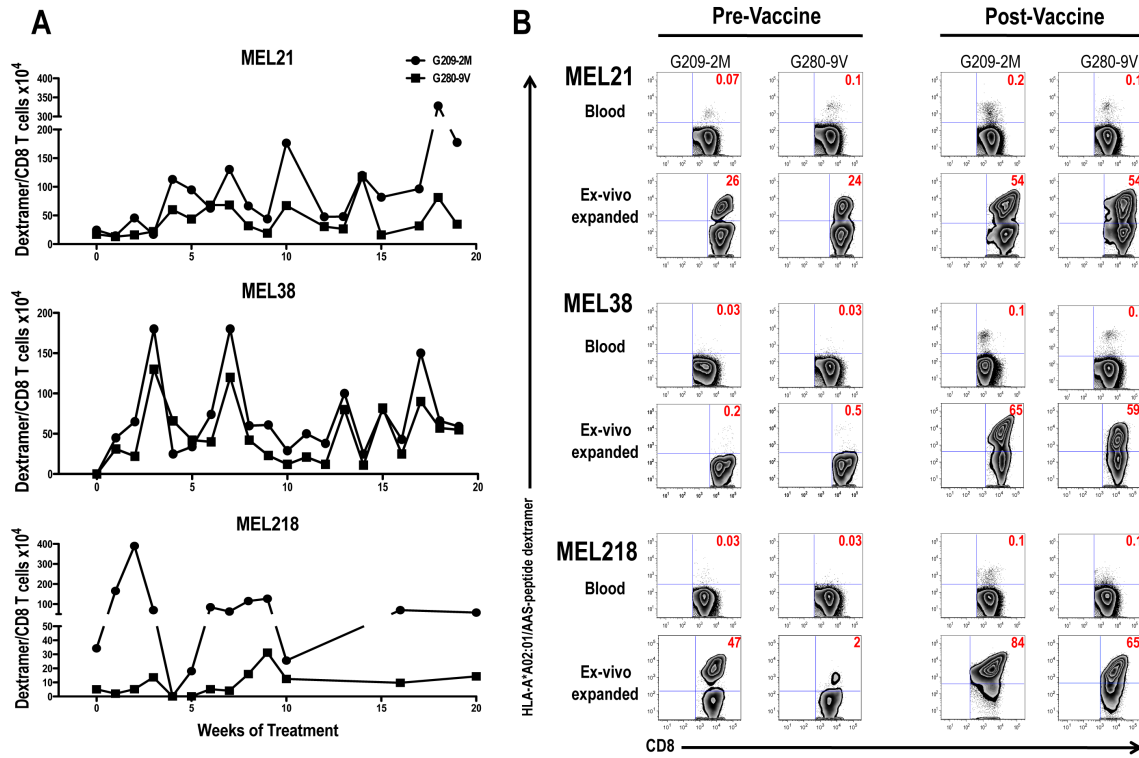


Fig. S5 Immunity to melanoma gp100 antigens. **(A)** Kinetics of immune responses to G209-2M and G280-9V peptides. Time is recorded in weeks (0 indicates pre-vaccination). Culture conditions and staining details are described in Methods. Antigen-specific numbers were calculated based on dextramer percentage and total live cell yields. **(B)** Frequency of G209-2M- and G280-9V-specific T cells in CD8+ populations isolated directly from PBMC samples and after ex-vivo expansion using autologous DC and artificial antigen presenting cells. Results are shown for samples obtained before vaccination (Pre-vaccine) and at peak post vaccination (Post-vaccine). Percentage of antigen-specific CD8+ T cells is indicated in the right upper quadrant of the plot. A representative experiment of 3 performed is shown.

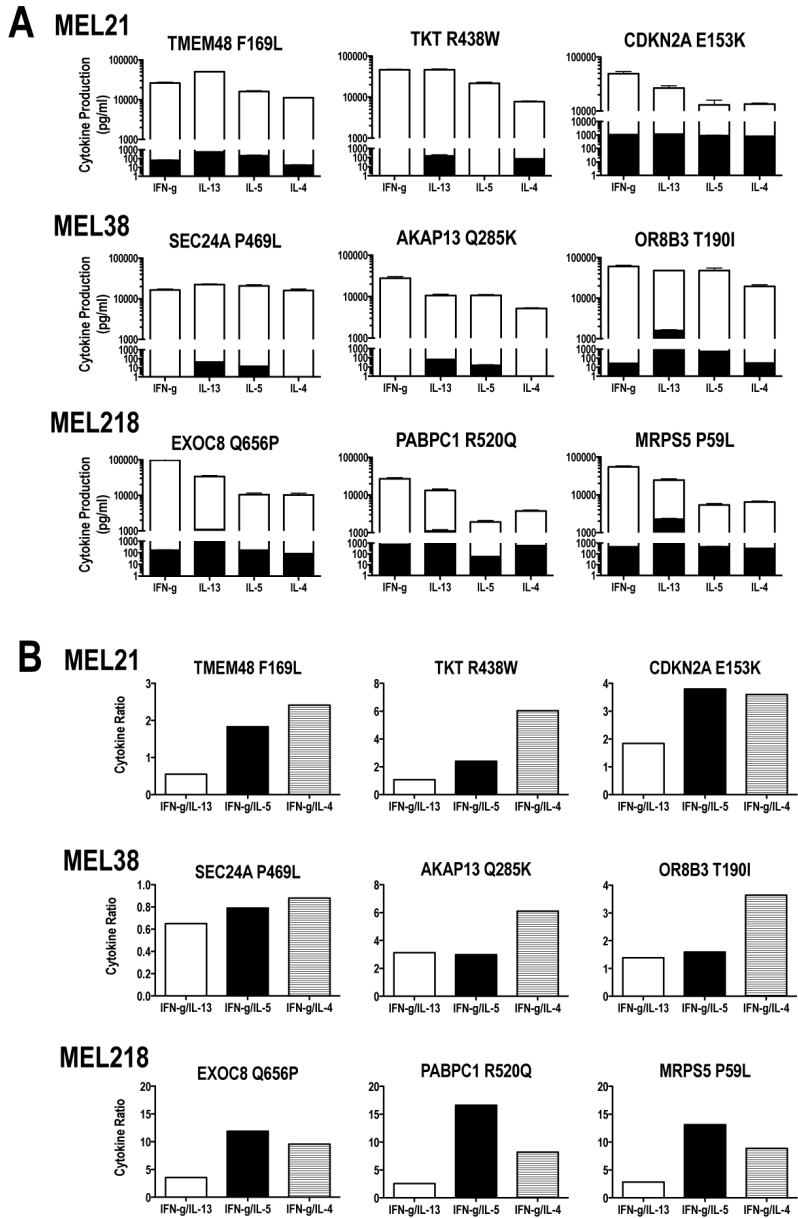


Fig. S6 Type 1 / Type 2 phenotype of neoantigen-specific CD8+ T cells. **(A)** Neoantigen-specific T cells were stimulated with artificial antigen presenting cells in the presence (open bar) or absence (closed bar) of AAS-peptide and supernatants were harvested at 24 h. Cytokine production was determined using MILLIPLEX® MAP Human Cytokine Panel I. Mean values +/- SD of duplicates are shown. Cytokine production by T cells in the absence of any stimuli was ≤ 100 pg/mL. A representative experiment of 2 performed is shown. **(B)** To compare production of Type 1 (IFN- γ) and Type 2 (IL-4, IL-5, IL-13) cytokines among neoantigen-specific T cells, a cytokine index was derived by dividing pg/mL IFN- γ by pg/mL IL-13, IL-5 or IL-4. IFN- γ /IL-13, IFN- γ /IL-5 and IFN- γ /IL-4 ratios above 1 are indicative of Type 1 phenotype. Results are representative of 2 experiments.

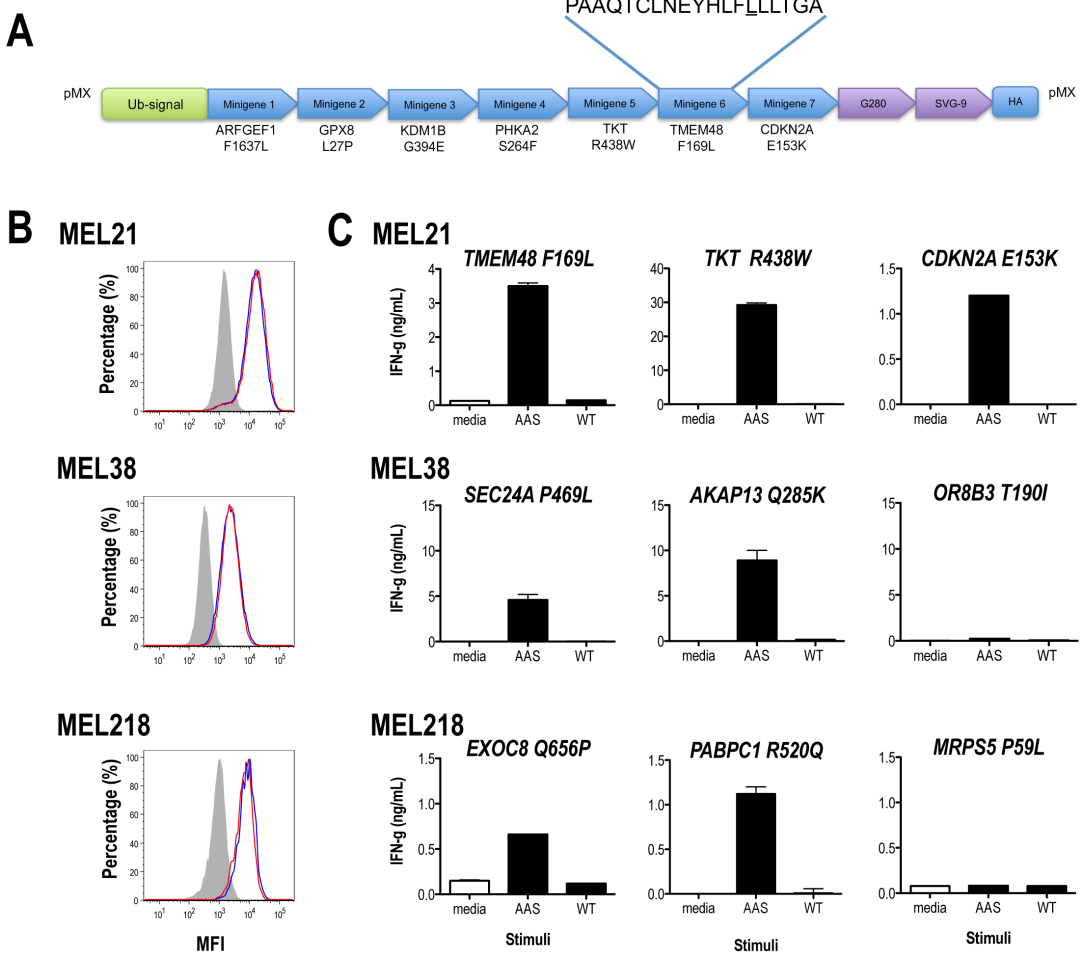


Fig. S7 Neoantigen processing and presentation. **(A)** Tandem mini-gene constructs (TMC) used for evaluating processing and presentation of neoantigens. The structure of a representative TMC (MEL21 AAS sequences) is shown. All constructs consisted of 19-21 mers encoding AAS- or WT- sequences for peptides included in vaccine. No spacers are present between sequences. A ubiquitination signal and 2 mini-gene controls (encoding G280 and WNV SVG9 peptides) were included to monitor processing and presentation. The amino acid sequence of a 21-mer encoding TMEM48 F169L is shown with mutated amino acid residue underlined. **(B)** Expression of AAS- and WT- TMC constructs was determined using a TCR-mimic monoclonal antibody that detects HLA-A*02:01/SVG9 (SVGGVFTSV) complexes (34). Results are shown for parental DM6 (shaded histogram) and DM6 cells expressing AAS- (red line) and WT (blue line) TMC constructs. A representative experiment of 4 performed is shown. **(C)** Neoantigen-specific CD8 T cells were co-cultured with DM6 expressing AAS- or WT- encoding TMC for 20 h and IFN- γ production determined by ELISA. T cells cultured with parental DM6 cells are indicated as media. Mean values +/- SD of duplicates are shown. Results are representative of 2 experiments performed.

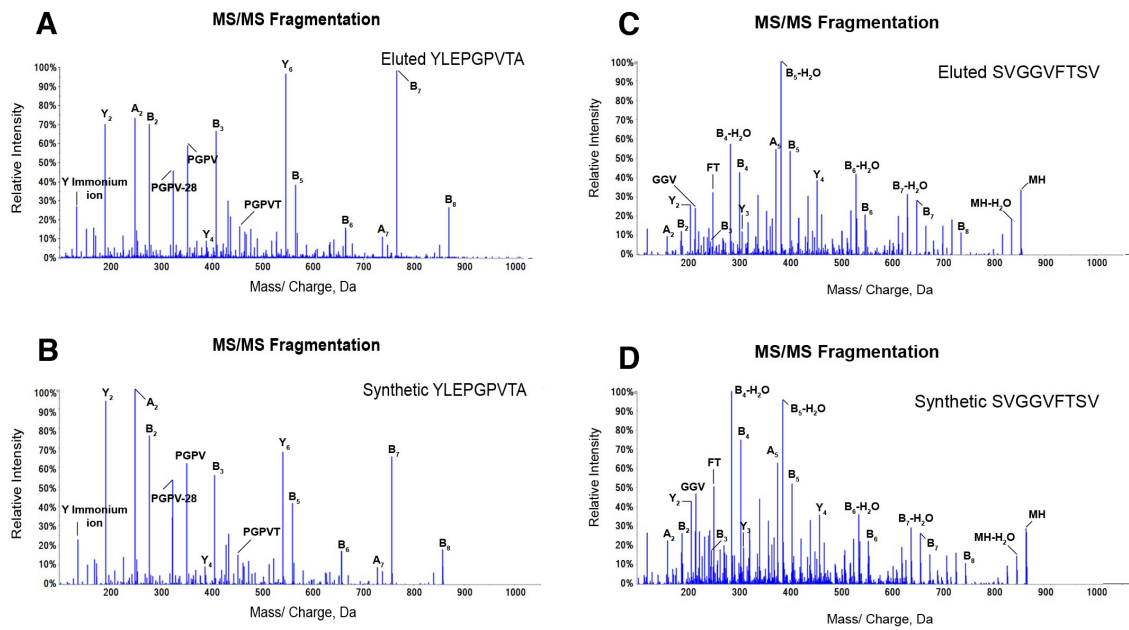


Fig. S8 Processing and presentation of melanoma G280 and WNV SVG9 peptide controls. MS/MS fragmentation pattern of **(A)** the peptide eluted from HLA-A*02:01 identified as YLEPGPVTA, and **(B)** the corresponding G280 synthetic peptide. MS/MS fragmentation pattern of **(C)** the peptide eluted from HLA-A*02:01 identified as SVGGVFTSV, and **(D)** the corresponding WNV SVG9 synthetic peptide.

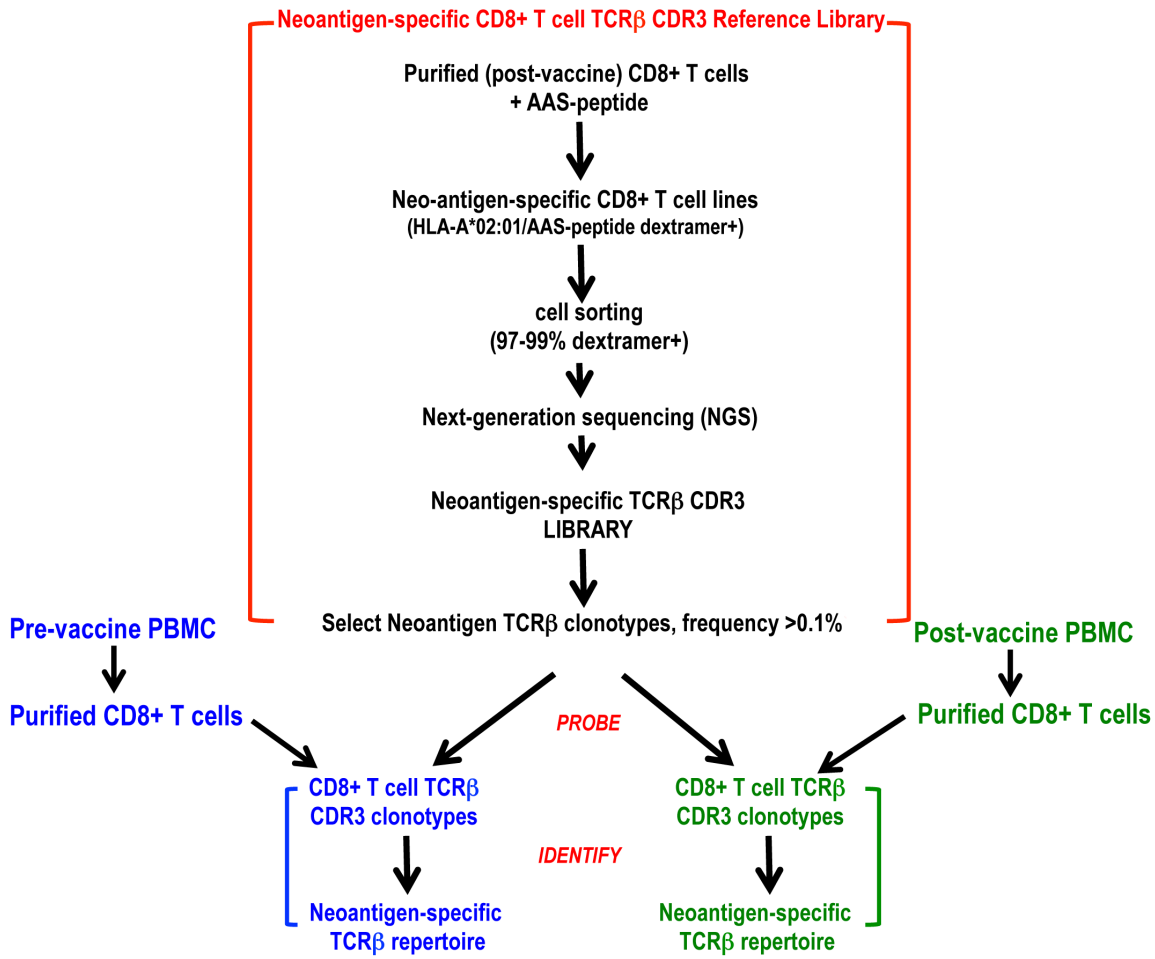


Fig. S9 Schematic diagram for analysis and identification of neoantigen-specific TCR β clonotypes in CD8+ T cell populations isolated from PBMC samples obtained Pre- and Post-vaccination.

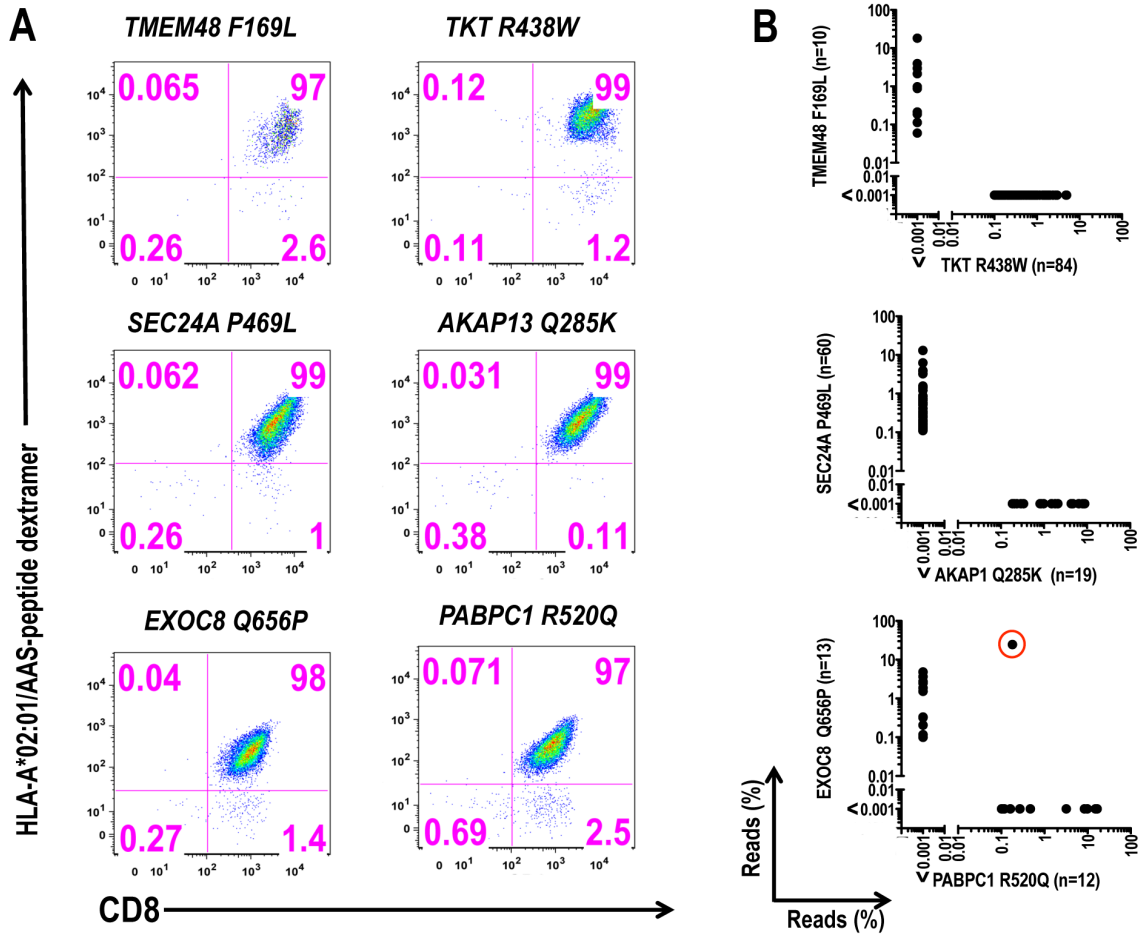


Fig. S10 Profiles of purified neoantigen-specific CD8⁺ T cells used for the generation of TCR β CDR3 reference libraries. **(A)** Purified CD8⁺ T cells isolated from PBMC obtained after vaccination were stimulated in an antigen-specific manner as described in Materials and Methods. Cells were stained using HLA-A*02:01/AAS-peptide dextramers and anti-CD8 monoclonal antibody; neoantigen-specific CD8⁺ T cells were sorted in a Sony SY3200 BSC Cell Sorter. Purity of post-sort populations is shown in dot plots (upper right quadrants, 97-99% purity). **(B)** Comparison of clonotype distribution in sorted/expanded dominant and subdominant neoantigen-specific CD8 T cells obtained from each of the indicated patients. These clonotypes represent the TCR β CDR3 reference libraries used for probing pre- and post-vaccine CD8⁺ T cell populations. Frequencies are shown as % of total reads. Reference library comprised clonotypes with frequencies of 0.1 or above (23). The total number of clonotypes in each antigen population is indicated in the x- and y- axis and CDR3 sequences are listed in Tables S6-S10. The one clonotype that overlapped between EXOC8 Q656P and PABPC1 R520Q (indicated by red circle) was excluded from analysis.

Table S4 –Analysis of HLA-A*02:01 restricted AAS-directed CD8+ T cell responses.

Patient	Hugo symbol	Amino Acid Substitution (AAS)	Mutated Peptide ^a	Predicted affinity (nM)	Experimental Affinity log[IC50, nM] ^b	Spontaneous Immunity ^c	Immunogenicity	Recognition of processed antigen	Antigenic Determinant ^d
MEL21	ARFGEF1 CDKN2A GPX8 KDM1B PHKA2 TKT TMEM48	F1637L E153K L27P G394E S264F R438W F169L	QTIDNIVFL KMIGNHLWV LLSIVECTV IIGAGPAEV* LLSIIFFPA AMFHSVPTV* CLNEYHFL <u>L</u>	67 14 52 111 23 4 23	3.19 3.18 3.09 3.82 3.90 2.35 3.09	No No No No No No Yes	No Yes No No No Yes Yes	Yes Yes	SUBDOMINANT SUBDOMINANT DOMINANT
MEL38	AKAP13 ARFGEF1 HSD17B7 OR8B3 PRKCDBP SEC24A UTRN	Q285K R782C H108Y T190I S153F P469L Q1058K	KLMNIQQKL FVSALCMFL YISKCWDXA QLSCISTV CLEPQTLAA FLYNLLTRV QLDKCSAFV	19 19 233 18 81 4 21	3.07 3.18 4.28 3.10 3.53 2.60 3.36	No No No No No Yes No	Yes No No Yes No Yes No	Yes No Yes	SUBDOMINANT CRYPTIC DOMINANT
MEL218	EXOC8 LARP7 MRPS5 MRPS17 PABPC1 SMOX SRP9	Q656P N515D P59L P167L R520Q K499N I64M	IILVAVPHV AVIDAYTEI HYASLSRV* VLLRALPVL MLGEQLPFL KLANPLPYT IMAHCIIDL	25 213 19 24 3 134 37	3.06 4.41 3.28 3.05 2.35 3.73 4.02	Yes No No No No No No	Yes No Yes No Yes No No	Yes No Yes	DOMINANT CRYPTIC SUBDOMINANT

^a Mutated residues are underlined and peptides that elicited immune responses are bolded in red (naturally-occurring) and blue (vaccine-induced).

* Indicates anchor-modified peptides at P9 (Tables S1-S3).

^b Affinity experimentally determined using fluorescence polarization-based competitive peptide-binding assay, high affinity binding peptides in this assay are log(IC₅₀; nM) <3.7 (11).

^c As determined by immune monitoring assay (Fig. 1B, Fig. S4B).

^d Antigenic determinant classification according to (18).

Table S5 –Tandem Mini-Gene Constructs (TMC)

Tumor	Gene	Mut AA Position	Nucleotide sequence*
MEL21	ARFGEF1	1637	CAGCTGGAGCTGATCCAGACGATAGACAACATCGTGGCTGCAACTAGTAAG
	GPX8	27	AAAGTTTCGCTGCTCTGCTCATTGCGGTGCACAGTGACACTTTTCCTT
	KDM1B	394	AACAAAGCGTATAATTATAGGAGCTGGCCAGCAGAAGTGGCAGCAGTAGACAA
	PHKA2	264	GAGATCGATGCTGGACTGCTTAGATAATCTTTCTGCTTTGCGGTAGAGGAT
	TKT	438	GCGCTGAAAGACCTGGTATGTTTGGTCACTGCCACAGTGACAGTCTCACAGGTGCC
	TMEM48	169	CCTGCAGCTCAGACCTGCTCAACAGATACCTGTTCTCACAGGTGCC
	CDKN2A	153	GCTGAGGGACCCCTCAAATGATAGCTAACCATCTGTTGATGCGAGTCGCCAT

Tumor	Gene	Mut AA Position	Nucleotide sequence*
MEL38	AKAP13	285	ACTGCCCTATTTAAGCTCATGAAATATCCAGCAAAGCTTATGAAAACAAATCTGAAG
	ARFGEF1	782	TTTAGCGAAAAGATTGTGAGCGCACTCTGCATGTTCTGAGGGATTCAAGCTGCCA
	PRKDCBP	153	CTGCCAGTCATGCGTCTTCCCCAAACTCTGCCGCTGAGGAGGGCGAGGTG
	SEC24A	469	GATGTCGAGAGGAGTTCTCTATAATCTGCTACACGCTCACGGAGAGCCACACGG
	UTRN	1058	GCTGATTGCAACGGCAGCTGGACAAATGAGCAGCTTACGCTAAATGAGATGAAACATA
	OR8B3	190	ATCCTGCCACTGCTGCAACTGTCATTTCTACCTACGTGAATGAAGTGTGGCCTC
	HSD17B7	108	TCCGAGATCAGACCATACTAGCAAGTGTGGACTATGCC

Tumor	Gene	Mut AA Position	Nucleotide sequence*
MEL218	MRPS17	167	ACAGTGGGGACATGTGCTGTCGGAGCACTGCCCTACTTCGAGAAAACACGTGAAG
	MRPS5	59	GGCACACGGGACACACATCTGATGCCAGCTTGAGCGCGCACTCCAAACACAGTGTGC
	SRP9	64	CAATCTCCGTATGATCATGCCCACTGTATCTCGACTTGTGGCACAGCGGGCCC
	LARP7	515	CCAGAGGACGCACAGGCACTGATCGACGCCCTACACCGAGATAAAACAGAAACATTGTGG
	EXOC8	656	GAATCCCTGGTCGAGATCATCTGGTAGCTGTTCCACATGTCATTACGCCCTAGGTGT
	SMOX	499	GGTGGCGATGTCGAAAAGCTGCCAACCTCTCCCTATACGAAATCAAGCAAACCGCG
	PABPC1	520	CCACAGGAGCAAAATGTTGGCGAACATTGTCAGGCTGATGCACCCG

Control Ag	Gene	Mut AA Position	Nucleotide sequence
G280	GP100	N/A	GTGGTGCACACACACTATCTCGAGCCGGGCCGTGACAGCCCAAGTAGTTCTGCAGGCC
SVG9	WNV	N/A	GCTTGGGATTCGGAGCGTGGGTGGCGTCTCACATGTTGCAAGGCAGTGCATCAG

* shown are nucleotide sequences encoding 19-21 amino acid long sequences containing amino acid substitutions targeted by peptides included in vaccine.

Table S6 – Reference TCR β CDR3 libraries from dominant TMEM48 F169L (MEL21)

CDR3 amino acid sequence	TCRBV	TCRBD	TCRBJ	Frequency	Read Counts
CASSQDLGGVYYGYTF	TCRBV04-01		TCRBJ01-02	18.24	494191
CSTLLAGGGDEQYV	TCRBV29-01	TCRBD02	TCRBJ02-07	3.96	107162
CASSPTGLGETQYF	TCRBV10-02	TCRBD01	TCRBJ02-05	2.97	80581
CSAPPGPLAHTQYF	TCRBV20	TCRBD02	TCRBJ02-03	2.14	58087
CASSFKGTGPQNQPQHF	TCRBV27-01	TCRBD01	TCRBJ01-05	0.98	26493
CASSFGGPPNTGELFF	TCRBV06	TCRBD02	TCRBJ02-02	0.88	23788
CASSIGPVNTEAFF	TCRBV19-01	TCRBD01	TCRBJ01-01	0.21	5787
CASSVAASPSGNTIYF	TCRBV09-01		TCRBJ01-03	0.19	5051
CASSPYRAGYEQYF	TCRBV03	TCRBD01	TCRBJ02-07	0.11	3056
CASSRTGITDTQYF	TCRBV03	TCRBD01	TCRBJ02-03	0.06	1619

TCRBV, TCRBD and TCRBJ are shown according to consensus nomenclature and CDR3 sequence for each clonotype indicated. Read counts indicates the number of times a give CDR3 sequence was found in the short term ex-vivo expanded neoantigen population. TCR β clonotypes with frequencies above 0.1% (>100-fold sequencing depth), in reference library, were set as a threshold for identification of neoantigen-specific TCR β CDR3 sequences within CD8+ T cell populations isolated from PBMC obtained pre- and post-vaccination.

Table S7 – Reference TCR β CDR3 libraries from subdominant TKT R438W neoantigen (MEL21)

CDR3 amino acid sequence	TCRBV	TCRBD	TCRBJ	Frequency	Read Counts
CASSIISAGGIYEQYF	TCRBV19-01	TCRBD02	TCRB ^J 02-07	4.97	112412
CASSISSEKLFF	TCRBV19-01	TCRBD02	TCRB ^J 01-04	4.79	108219
CASSLVVGLALEQYF	TCRBV12	TCRBD02	TCRB ^J 02-07	2.96	66848
CASSFWGLSTEAFF	TCRBV12	TCRBD02	TCRB ^J 01-01	2.75	62085
CASSSDLYEQYF	TCRBV05-04		TCRB ^J 02-07	2.38	53716
CASSQEVGSGNTIYF	TCRBV04-03		TCRB ^J 01-03	2.00	45241
CASSAGGGGNTIYF	TCRBV07-08	TCRBD01	TCRB ^J 01-03	1.97	44623
CASSIAGGYEQYV	TCRBV19-01	TCRBD01	TCRB ^J 02-07	1.86	42081
CSVVGGLLEAFF	TCRBV29-01	TCRBD02	TCRB ^J 01-01	1.84	41524
CASSSDWGLMNTTEAFF	TCRBV05-06	TCRBD01	TCRB ^J 01-01	1.78	40297
CASSAVDRVTSYNEQOFF	TCRBV27-01	TCRBD01	TCRB ^J 02-01	1.67	37852
CASSLIAGNSTQYF	TCRBV12	TCRBD02	TCRB ^J 02-03	1.64	37136
CASRLTAGEYQETQYF	TCRBV12-02	TCRBD02	TCRB ^J 02-05	1.64	36999
CASSLWDYGYTF	TCRBV05-06		TCRB ^J 01-02	1.59	35919
CASSLWGVGTEAFF	TCRBV12	TCRBD02	TCRB ^J 01-01	1.54	34759
CASSYFGVNSPLHF	TCRBV06	TCRBD02	TCRB ^J 01-06	1.48	33424
CATSALAGQGRDEQFF	TCRBV24	TCRBD01	TCRB ^J 02-01	1.42	32032
CASSRLAGTDQYF	TCRBV12	TCRBD02	TCRB ^J 02-03	1.36	30644
CASSFPYGLNTEAFF	TCRBV06	TCRBD02	TCRB ^J 01-01	1.59	36045
CASSVLAGGLDTQYF	TCRBV10-02	TCRBD02	TCRB ^J 02-03	1.15	26035
CASSYMLQTFTNEAFF	TCRBV06		TCRB ^J 01-01	1.00	22716
CASSPGLLAGGSSWEQYF	TCRBV07-02	TCRBD02	TCRB ^J 02-05	0.99	22276
CASTSTPQVGQPQPHF	TCRBV27-01	TCRBD01	TCRB ^J 01-05	0.95	21583
CASKGLAGAYTDTQYF	TCRBV12	TCRBD02	TCRB ^J 02-03	0.87	19584
CASSLQGNEQYF	TCRBV07-08		TCRB ^J 02-07	0.86	19499
CASSFTAGLNTEAFF	TCRBV12	TCRBD01	TCRB ^J 01-01	0.83	18659
CASSLWVGLGTEAFF	TCRBV28-01		TCRB ^J 01-01	0.80	18100
CASSGLLSGESF	TCRBV07-08	TCRBD02	unresolved	0.78	17740
CASSKLAGGLDTQYF	TCRBV10-02	TCRBD02	TCRB ^J 02-03	0.78	17662
CASTHTRGLNTEAFF	TCRBV12	TCRBD01	TCRB ^J 01-01	0.77	17470
CASSIQQEEQETQYF	TCRBV03	TCRBD01	TCRB ^J 02-05	0.76	17163
CASSLEIVGETEAFF	TCRBV05-06		TCRB ^J 01-01	0.68	15460
CASSISGGYEQYV	TCRBV19-01	TCRBD01	TCRB ^J 02-07	0.68	15403
CSARTLAGPTDTQYF	TCRBV20	TCRBD02	TCRB ^J 02-03	0.65	14669
CASSDLLTGELFF	TCRBV06-01	TCRBD02	TCRB ^J 02-02	0.58	13155
CASSSCLAGLYM	TCRBV07-08	TCRBD02	TCRB ^J 02-03	0.55	12339
CASSHRTITDEETQYF	TCRBV23-01	TCRBD01	TCRB ^J 02-05	0.54	12253
CASSVPYGLNTEAFF	TCRBV06		TCRB ^J 01-01	0.49	11037
CASSLDLYEQYF	TCRBV05-04		TCRB ^J 02-07	0.44	9958
CASSWTGFGLNTEAFF	TCRBV06	TCRBD01	TCRB ^J 01-01	0.44	9860
CASSLITGGLSYEQYF	TCRBV12	TCRBD01	TCRB ^J 02-07	0.42	9469
CASSWTWGMNTEAFF	TCRBV28-01	TCRBD01	TCRB ^J 01-01	0.40	9127
CASSELWGAQDNEOFF	TCRBV10-02	TCRBD02	TCRB ^J 02-01	0.39	8722
CASSFTITGLHYEQYF	TCRBV28-01	TCRBD02	TCRB ^J 02-07	0.38	8644
CASQAQTOPOHF	TCRBV20	TCRBD01	TCRB ^J 01-05	0.38	8478
CASSLVVGLAETQYF	TCRBV27-01		TCRB ^J 02-05	0.35	7817
CASSFSGLLTHEQYV	TCRBV06	TCRBD02	TCRB ^J 02-07	0.35	7808
CASSLIGAGEQYF	TCRBV07-08		TCRB ^J 02-07	0.33	7414
CASSPIFGLTNEQYF	TCRBV02-01	TCRBD02	TCRB ^J 02-07	0.31	6910
CASSYYFGGEQFF	TCRBV06	TCRBD02	TCRB ^J 02-01	0.30	6856
CASSQDWGLNYEQYF	TCRBV04-01		TCRB ^J 02-07	0.30	6776
CASSTSGGYEQYF	TCRBV19-01	TCRBD02	TCRB ^J 02-07	0.28	6396
CASSRLAGGLDTQYF	TCRBV10-02	TCRBD02	TCRB ^J 02-03	0.28	6392
CASSGLITDTQYF	TCRBV19-01	TCRBD02	TCRB ^J 02-03	0.26	5848
CSARELAQFOETQYF	TCRBV20	TCRBD02	TCRB ^J 02-05	0.25	5732
CSPIRGIEQOV	TCRBV20-01	TCRBD02	TCRB ^J 02-07	0.24	5486
CAIGPOGGFYEOYF	TCRBV10-02	TCRBD01	TCRB ^J 02-07	0.24	5364
CATSSAILAGVKETQYF	TCRBV15-01	TCRBD02	TCRB ^J 02-05	0.24	5313
CASSEGVGLAFEQOFF	TCRBV02-01	TCRBD02	TCRB ^J 02-01	0.23	5254
CAIGLAGAYEQYF	TCRBV10-03	TCRBD02	TCRB ^J 02-07	0.23	5123
CASSSWTGLSLSFYGYTF	TCRBV28-01	TCRBD01	TCRB ^J 01-02	0.22	5077
CASSEPEGTVEAFF	TCRBV02-01	TCRBD02	TCRB ^J 01-01	0.21	4771
CSVEEGIDEQYF	TCRBV29-01		TCRB ^J 02-07	0.20	4627
CASSILGAGEQOFF	TCRBV07-08	TCRBD02	TCRB ^J 02-01	0.20	4549
CASSFFQGGTGTNTIYF	TCRBV07-08	TCRBD02	TCRB ^J 01-03	0.20	4505
CASSLALALPYEQYF	TCRBV12	TCRBD02	TCRB ^J 02-07	0.18	4029
CASSSPOTGLAITEGELFF	TCRBV19-01	TCRBD02	TCRB ^J 02-02	0.18	3969
CASSQTHPPGELFF	TCRBV04-03		TCRB ^J 02-02	0.17	3928
CASSISAGYEQYV	TCRBV19-01	TCRBD02	TCRB ^J 02-07	0.16	3684
CASSVDGAYNEQFF	TCRBV09-01	TCRBD02	TCRB ^J 02-01	0.16	3650
CAPFGVNWLDPHSGNTIYF	TCRBV30-01		TCRB ^J 01-03	0.15	3435
CASSFTWGLNTEAFF	TCRBV12		TCRB ^J 01-01	0.14	3276
CASSYYFSYEQYF	TCRBV06		TCRB ^J 02-07	0.14	3150
CASSSDRGLPSGNTIYF	TCRBV28-01	TCRBD01	TCRB ^J 01-03	0.13	2973
CSAHEGLEQVF	TCRBV20-01		TCRB ^J 02-07	0.13	2906
CASSASWTDDYYGYTF	TCRBV27-01	TCRBD01	TCRB ^J 01-02	0.13	2902
CASSTGIGSYEQYF	TCRBV06		TCRB ^J 02-07	0.12	2718
CASSLWYNQPOHFF	TCRBV27-01		TCRB ^J 01-05	0.12	2715
CASSPLAAPGSFETQYF	TCRBV06	TCRBD02	TCRB ^J 02-05	0.11	2420
CASSVDGDYNEQFF	TCRBV09-01	TCRBD02	TCRB ^J 02-01	0.11	2406
CASSPTPSGLWELFF	TCRBV12	TCRBD02	TCRB ^J 02-02	0.11	2400
CASSTGTGLNTEAFF	TCRBV02-01	TCRBD01	TCRB ^J 01-01	0.10	2348
CATSALPQETTDTQYF	TCRBV24	TCRBD01	TCRB ^J 02-03	0.10	2267
CASSLVGGLSNQPOHFF	TCRBV27-01	TCRBD02	TCRB ^J 01-05	0.10	2265

TCRBV, TCRBD and TCRBJ are shown according to consensus nomenclature and CDR3 sequence for each clonotype indicated. Read counts indicates the number of times a give CDR3 sequence was found in the short term ex-vivo expanded neoantigen population. TCR β clonotypes with frequencies above 0.1% (>100-fold sequencing depth), in reference library, were set as a threshold for identification of neoantigen-specific TCR β CDR3 sequences within CD8+ T cell populations isolated from PBMC obtained pre- and post-vaccination.

Table S8 – Reference TCR β CDR3 libraries from dominant SEC24A P469L neoantigen (MEL38)

CDR3 amino acid sequence	TCRBV	TCRBD	TCRBJ	Frequency	Read Counts
CASSQQAGGITYNEQFF	TCRBV03	TCRBD01	TCRBJ02-01	13.04	142392
CASSYSTAGOPQHF	TCRBV06-05	TCRBD01	TCRBJ01-05	6.25	68241
CASSPTGAGYEQYF	TCRBV06-05	TCRBD01	TCRBJ02-07	3.96	43243
CASSLLSGSTEAFF	TCRBV28-01	TCRBD02	TCRBJ01-01	3.83	41830
CASSYGTSTNEQFF	TCRBV06-05	TCRBD02	TCRBJ02-01	3.26	35641
CASSQGDGTDQYF	TCRBV03	TCRBD01	TCRBJ02-03	1.57	17192
CASSFSNQPQHF	TCRBV28-01		TCRBJ01-05	1.57	17171
CASSGGQGTQPOQHF	TCRBV28-01		TCRBJ01-05	1.49	16310
CASSSYSGAGOPQHF	TCRBV06-05	TCRBD01	TCRBJ01-05	1.42	15495
CASSLLQGAESPLHF	TCRBV13-01	TCRBD01	TCRBJ01-06	1.39	15226
CASSPQDRGPNYGYTF	TCRBV28-01	TCRBD01	TCRBJ01-02	1.21	13219
CASSFDYSYEQYF	TCRBV05-04	TCRBD02	TCRBJ02-07	0.88	9558
CAAGGVNQPQHF	TCRBV28-01		TCRBJ01-05	0.84	9144
CASSLLLAGELFF	TCRBV06-05	TCRBD02	TCRBJ02-02	0.76	8282
CASSPSSPYEQYF	TCRBV12	TCRBD02	TCRBJ02-07	0.72	7894
CASSEGTDTQYF	TCRBV10-02		TCRBJ02-03	0.67	7299
CASG1ISNQPQHF	TCRBV28-01		TCRBJ01-05	0.66	7225
CASSLDPPFDRQNYGYTF	TCRBV28-01	TCRBD01	TCRBJ01-02	0.59	6456
CASSYGDAYNEQFF	TCRBV06-05		TCRBJ02-01	0.59	6440
CATMGTGGSLYYGYTF	TCRBV28-01	TCRBD01	TCRBJ01-02	0.59	6433
CASSVSNQPQHF	TCRBV28-01		TCRBJ01-05	0.58	6305
CASSEFTGGYNEQFF	TCRBV28-01	TCRBD02	TCRBJ02-01	0.55	6055
CASSLYRANTGELFF	TCRBV28-01	TCRBD01	TCRBJ02-02	0.53	5747
CASSLLTSLTDQYF	TCRBV06-05	TCRBD02	TCRBJ02-03	0.51	5617
CASSSKSKGSPHLF	TCRBV21-01		TCRBJ01-06	0.42	4580
CASSLAGQGPNSPLHF	TCRBV05-06	TCRBD01	TCRBJ01-06	0.41	4470
CASSPTGAGOPQHF	TCRBV06-05	TCRBD01	TCRBJ01-05	0.40	4417
CASSSGTGSQSDTQYF	TCRBV28-01	TCRBD02	TCRBJ02-03	0.35	3791
CASSFSGPSPQHF	TCRBV12		TCRBJ01-05	0.33	3592
CASNLOGLDYEQYF	TCRBV12	TCRBD01	TCRBJ02-07	0.32	3519
CASSLGQGNQPQHF	TCRBV28-01	TCRBD01	TCRBJ01-05	0.32	3486
CASSFWGANEKLF	TCRBV28-01	TCRBD02	TCRBJ01-04	0.32	3474
CASSYSVGVNTEAFF	TCRBV06-05	TCRBD02	TCRBJ01-01	0.31	3419
CASRYRAAPNQPQHF	TCRBV28-01	TCRBD01	TCRBJ01-05	0.30	3235
CASSQDAGGVFGNTIYF	TCRBV03	TCRBD02	TCRBJ01-03	0.27	2894
CASSLYSNQPQHF	TCRBV28-01		TCRBJ01-05	0.25	2744
CATAPINSPLHF	TCRBV28-01	TCRBD02	TCRBJ01-06	0.24	2636
CASSPPNNQPQHF	TCRBV28-01		TCRBJ01-05	0.21	2262
CASSFFNNQPQHF	TCRBV28-01	TCRBD02	TCRBJ01-05	0.21	2255
CASGVSNQPQHF	TCRBV28-01	TCRBD01	TCRBJ01-05	0.20	2180
CASSYESNYGYTF	TCRBV06	TCRBD02	TCRBJ01-02	0.19	2093
CASSLDVATNEKLFF	TCRBV06-05		TCRBJ01-04	0.18	2018
CSDSSTGGAGFTF	TCRBV29-01	TCRBD01	TCRBJ01-02	0.17	1868
CASSESGGGYRWEAFF	TCRBV10-01	TCRBD02	TCRBJ01-01	0.17	1839
CASSEGPGSYTF	TCRBV09-01		TCRBJ01-02	0.17	1838
CASSPGLGEQYF	TCRBV28-01	TCRBD02	TCRBJ02-07	0.16	1777
CASSLEGVYGYTF	TCRBV06		TCRBJ01-02	0.16	1758
CASTIGPGITDQYF	TCRBV05-06		TCRBJ02-03	0.16	1715
CASSPRDRGPRSPQHF	TCRBV28-01	TCRBD01	TCRBJ01-05	0.16	1714
CASSRTGAGEKLFF	TCRBV06-05	TCRBD01	TCRBJ01-04	0.16	1705
CASSLGIAAGPYNEQFF	TCRBV07-06	TCRBD02	TCRBJ02-01	0.15	1634
CAGGLLNQPQHF	TCRBV28-01	TCRBD02	TCRBJ01-05	0.14	1520
CASSLGQGAQPQHF	TCRBV28-01	TCRBD01	TCRBJ01-05	0.14	1497
CASSPMNTEAFF	TCRBV28-01	TCRBD02	TCRBJ01-01	0.14	1493
CASSLSSHGHTF	TCRBV28-01	TCRBD02	TCRBJ01-02	0.13	1397
CASSFATVGKEKLFF	TCRBV06-05	TCRBD01	TCRBJ01-04	0.12	1364
CASTLYTGDNEQFF	TCRBV06-05	TCRBD02	TCRBJ02-01	0.12	1358
CASSYSAGGYGYTF	TCRBV06-05	TCRBD01	TCRBJ01-02	0.12	1310
CASSYQGGSQQPQHF	TCRBV28-01	TCRBD01	TCRBJ01-05	0.11	1212
CASSPLNTEAFF	TCRBV19-01		TCRBJ01-01	0.11	1198
CASSWSNQPQHF	TCRBV28-01		TCRBJ01-05	0.10	1072

TCRBV, TCRBD and TCRBJ are shown according to consensus nomenclature and CDR3 sequence for each clonotype indicated. Read counts indicates the number of times a give CDR3 sequence was found in the short term ex-vivo expanded neoantigen population. TCR β clonotypes with frequencies above 0.1% (>100-fold sequencing depth), in reference library, were set as a threshold for identification of neoantigen-specific TCR β CDR3 sequences within CD8+ T cell populations isolated from PBMC obtained pre- and post-vaccination.

Table S9 – Reference TCR β CDR3 libraries from subdominant AKAP13 Q285K neoantigen (MEL38)

CDR3 amino acid sequence	TCRBV	TCRBD	TCRBJ	Frequency	Read Counts
CASSPVTGGDNSPLHF	TCRBV13-01	TCRBD01	TCRBJ01-06	8.80	69934
CASSSGNYEQYF	TCRBV13-01		TCRBJ02-07	8.52	67687
CASSLGLSGAYNEQFF	TCRBV13-01	TCRBD01	TCRBJ02-01	7.87	62566
CAWSVASGNEQFF	TCRBV30-01	TCRBD02	TCRBJ02-01	6.44	51166
CASSWGQGGYEQYF	TCRBV13-01	TCRBD01	TCRBJ02-07	4.66	37068
CAWSVGVSNQPQHF	TCRBV30-01		TCRBJ01-05	4.36	34646
CASSLGQGGELFF	TCRBV13-01	TCRBD01	TCRBJ02-02	4.30	34205
CASSLGNYEQYF	TCRBV13-01	TCRBD01	TCRBJ02-07	2.10	16658
CAWSAGTGGNEKLFF	TCRBV30-01	TCRBD01	TCRBJ01-04	1.82	14434
CAWSVAGGHEQYF	TCRBV30-01	TCRBD01	TCRBJ02-07	1.49	11869
CASSLGQGYEQYF	TCRBV13-01	TCRBD01	TCRBJ02-07	0.98	7807
CASSFGQRETEAFF	TCRBV05-06		TCRBJ01-01	0.86	6805
CASSQGTGVTEAFF	TCRBV13-01	TCRBD01	TCRBJ01-01	0.85	6761
CASSFGTGVEQYF	TCRBV06-05	TCRBD01	TCRBJ02-07	0.81	6446
CASSLNPDQTQYF	TCRBV05-06		TCRBJ02-03	0.33	2657
CAWSPGQGGTNEKLFF	TCRBV30-01	TCRBD01	TCRBJ01-04	0.29	2319
CAWSAYTGELFF	TCRBV30-01	TCRBD01	TCRBJ02-02	0.23	1846
CAWSVGAGVGEQYF	TCRBV30-01	TCRBD02	TCRBJ02-07	0.20	1625
CAWSGDRPLAFF	TCRBV30-01		TCRBJ01-01	0.18	1470

TCRBV, TCRBD and TCRBJ are shown according to consensus nomenclature and CDR3 sequence for each clonotype indicated. Read counts indicates the number of times a give CDR3 sequence was found in the short term ex-vivo expanded neoantigen population. TCR β clonotypes with frequencies above 0.1% (>100-fold sequencing depth), in reference library, were set as a threshold for identification of neoantigen-specific TCR β CDR3 sequences within CD8+ T cell populations isolated from PBMC obtained pre- and post-vaccination.

Table S10 – Reference TCR β CDR3 libraries from dominant EXOC8 Q656P and subdominant PABPC1 R520Q neoantigens (MEL218)

EXOC8 Q656P					
CDR3 amino acid sequence	TCRBV	TCRBD	TCRBJ	Frequency	Read Counts
CASSVGLSETTALYNEQFF	TCRBV25	TCRBD02	TCRBJ02-01	4.85	15597
CASSLEVVOETQYF	TCRBV11-02		TCRBJ02-05	3.64	11717
CSARDPASWGEKLFF	TCRBV20		TCRBJ01-04	2.75	8846
CASSVAGLQAEQYF	TCRBV09-01		TCRBJ02-07	2.5	8039
CASSYEQGSYEQYF	TCRBV06-05	TCRBD01	TCRBJ02-07	1.87	6014
CASSFGPLGMWAEAFF	TCRBV06		TCRBJ01-01	1.53	4914
CASSYLSVQETQYF	TCRBV11-02	TCRBD02	TCRBJ02-05	0.33	1061
CASSLETGYGEQYF	TCRBV05-05	TCRBD01	TCRBJ02-07	0.33	1052
CASSVFGLAGAEQYF	TCRBV09-01	TCRBD02	TCRBJ02-07	0.32	1033
CASSEFGGGSPDTQYF	TCRBV09-01	TCRBD02	TCRBJ02-03	0.21	661
CASSVYGGAEAFF	TCRBV09-01	TCRBD02	TCRBJ01-01	0.12	370
CASSTYGLAGETQYF	TCRBV09-01	TCRBD02	TCRBJ02-05	0.1	322

PABPC1 R520Q					
CDR3 amino acid sequence	TCRBV	TCRBD	TCRBJ	Frequency	Read Counts
CSVENRVIYGYTF	TCRBV29-01	TCRBD01	TCRBJ01-02	16.65	28165
CSVEDPTFYGYTF	TCRBV29-01		TCRBJ01-02	15.13	25599
CASSLGSSGNTIYF	TCRBV09-01		TCRBJ01-03	9.83	16628
CSVEGQIAGKYGYTF	TCRBV29-01		TCRBJ01-02	8.42	14240
CASSYGTSGTEQFF	TCRBV07-06	TCRBD02	TCRBJ02-01	3.20	5412
CSVEDGAAKQIYGYTF	TCRBV29-01		TCRBJ01-02	0.47	797
CASSVEYSNQPQHF	TCRBV02-01	TCRBD02	TCRBJ01-05	0.27	457
CSVEDRVNYGYTF	TCRBV29-01	TCRBD01	TCRBJ01-02	0.16	275
CASSQWSSTNEKLFF	TCRBV14-01		TCRBJ01-04	0.12	199
CARNHDRDRLYEQYF	TCRBV02-01	TCRBD01	TCRBJ02-07	0.11	185
CASSSWGTSDEQYF	TCRBV07-09	TCRBD02	TCRBJ02-07	0.10	172

TCRBV, TCRBD and TCRBJ are shown according to consensus nomenclature and CDR3 sequence for each clonotype indicated. Read counts indicates the number of times a give CDR3 sequence was found in the short term ex-vivo expanded neoantigen population. TCR β clonotypes with frequencies above 0.1% (>100-fold sequencing depth), in reference library, were set as a threshold for identification of neoantigen-specific TCR β CDR3 sequences within pre- and post-vaccine CD8+ T cell populations isolated from PBMC obtained pre- and post-vaccination.